Development 136, 1605-1611 (2009) doi:10.1242/dev.035436

Floral stem cell termination involves the direct regulation of *AGAMOUS* by PERIANTHIA

Pradeep Das[1,2,*], Toshiro Ito[1,3], Frank Wellmer[1,4], Teva Vernoux[2], Annick Dedieu[2], Jan Traas[2] and Elliot M. Meyerowitz[1,*]

In *Arabidopsis*, the population of stem cells present in young flower buds is lost after the production of a fixed number of floral organs. The precisely timed repression of the stem cell identity gene *WUSCHEL* (*WUS*) by the floral homeotic protein AGAMOUS (AG) is a key part of this process. In this study, we report on the identification of a novel input into the process of floral stem cell regulation. We use genetics and chromatin immunoprecipitation assays to demonstrate that the bZIP transcription factor PERIANTHIA (PAN) plays a role in regulating stem cell fate by directly controlling *AG* expression and suggest that this activity is spatially restricted to the centermost region of the *AG* expression domain. These results suggest that the termination of floral stem cell fate is a multiply redundant process involving loci with unrelated floral patterning functions.

KEY WORDS: AGAMOUS, Flower development, Stem cells, *Arabidopsis*

INTRODUCTION

In *Arabidopsis*, the indeterminate shoot apical meristem (SAM) produces organs such as leaves and flowers throughout the life of the plant. By contrast, the determinate floral meristem (FM), from which flowers are derived, produces a stereotypical number of floral organs: four sepals, four petals, six stamens and two carpels. Underlying the different behaviors of these two meristematic tissues are the different properties of their respective stem cell populations. In the SAM, as well as in the FM, the expression of the homeodomain gene *WUSCHEL* (*WUS*) in a small group of cells at the center of the structures, the so-called stem cell organizing center, is essential for maintaining the pool of stem cells. In the FM, once the correct numbers of floral organs have formed, *WUS* is quickly downregulated and the stem cells lost (Laux et al., 1996; Mayer et al., 1998).

The floral identity regulator LEAFY (LFY) (Schultz and Haughn, 1991; Weigel et al., 1992) activates the expression of the homeotic gene *AGAMOUS* (*AG*) in the center of young flower buds, and the AG gene product then acts to downregulate *WUS*, leading to a loss of stem cell activity (Busch et al., 1999; Lenhard et al., 2001; Lohmann et al., 2001; Parcy et al., 1998). However, loss of LFY function only leads to a delay in the onset of *AG* expression, and not to its absence (Weigel and Meyerowitz, 1993), suggesting that other factors also play a role in the early activation of *AG*. One of these factors was recently shown to be WUS itself, which directly binds *AG* regulatory sequences in combination with LFY (Lohmann et al., 2001). Flowers mutant for *AG* display stem cell maintenance phenotypes, resulting in the formation of flowers within flowers, and also show homeotic transformations of stamens to petals (Bowman et al., 1989). It has been suggested that these are functionally distinct activities of AG (Mizukami and Ma, 1995; Sieburth et al., 1995), yet not much is known about how this is regulated: whether AG is regulated at the RNA level, for example, via the regulation of *AG* expression in specific floral domains, or at the protein level, through interactions between AG and other spatially restricted molecules. Furthermore, it is unclear how AG shuts down *WUS* expression and thus the floral stem cell population (Laux et al., 1996; Mayer et al., 1998).

In this study, we report on the identification of a novel input into the process of floral stem cell arrest and suggest that this activity is spatially restricted to the centermost region of the *AG* expression domain.

MATERIALS AND METHODS

Mutagenesis

pan-3 seeds (10,000-15,000; in the L-*er* accession) were treated with a 0.3% (v/v) aqueous solution of ethyl methanesulfonate (Sigma) in a volume of 15 ml for 10 hours, then washed with water for 8 hours (with hourly changes) before being resuspended in a 0.15% (v/v) agar solution and sowed on soil 1 cm apart. Seeds from M1 plants were harvested individually and 20-30 M2 plants per M1 line (~1000) were screened for altered floral phenotypes, which were reconfirmed in the M3 generation. Ten putative modifiers were retained after re-screening. To identify the mutation in the novel *lfy* allele, the genomic coding region was amplified in two fragments of 1.3 kb and 1.4 kb by PCR (using Ex Taq, Takara) and sequenced. The mutation was found to be a nonsense mutation (Q162Stop), similar to all published null alleles.

Plasmid constructs and sequences

Details of primers available upon request. All PCR amplifications were carried out using the Phusion high fidelity polymerase (Finnzymes). All constructs were sequenced. To construct the *PAN* repressor domain chimeric fusion, we first annealed complementary oligonucleotides carrying the enhanced SUPERMAN repressor domain motif flanked by *Bam*HI and *Bgl*II sites, and ligated this to the pGEM-T EZ cloning vector (Promega), to yield pGEM-SRDX. The *PAN* cDNA was PCR-amplified, digested with *Kpn*I and *Bgl*II and cloned into the *Kpn*I and *Bam*HI sites of pGEM-SRDX to yield pPD64.1. The *PAN-RD* fragment was extracted with *Bam*HI and *Bgl*II, and cloned into pBJ36 (Gleave, 1992) carrying either the *p35S*, *pPAN* or *pAP1*(*1.7-kb*) promoters to yield pPD66.1, pPD199.2 or pPD143.1 respectively. The *PAN* promoter was PCR-amplified from the L-*er* accession and cloned into pBJ36 using the *Sal*I and *Kpn*I sites. *pAP1*(*1.7-kb*) was a kind gift of Dr Marty Yanofsky (University of California, San Diego, CA, USA). The promoter-*PAN-RD* fragments were then extracted from pBJ36 using *Not*I and ligated to the plant transformation vector pML BART (Eshed et al., 2001) yielding pPD74.1, pPD218.1 or pPD171.20, respectively.

[1]Division of Biology 156-29, California Institute of Technology, Pasadena, California 91125, USA. [2]Laboratoire RDP, Ecole Normale Supérieure de Lyon, 46 allée d'Italie, 69007 Lyon, France. [3]Temasek Life Sciences Laboratory, National University of Singapore, Singapore 117604, Singapore. [4]Smurfit Institute of Genetics, Trinity College Dublin, College Green, Dublin 2, Ireland.

*Authors for correspondence (e-mails: pradeep.das@ens-lyon.fr; meyerow@its.caltech.edu)

Accepted 16 March 2009

For the ethanol-inducible version of *PAN-RD* under the control of the *PAN* promoter, we used the MultiSite Gateway Three-Fragment Vector Construction Kit (Invitrogen) to generate a single plasmid harboring the two components. We PCR-amplified a fragment of the *LFY::alcR--alcA::ER-GFP* pGreen binary vector (gift of Patrick Laufs; INRA, Versailles, France); the *alcR* gene harboring a 3′ *nos* terminator, followed by a *35S* terminator in an inverted orientation. This fragment was recombined with the pDONR 221 vector to generate pENTR-*alcR*-2xT. We also modified a destination vector (pGreen 0229; gift of Philip Benfey; Duke University, Durham, NC, USA) by inserting the chimeric promoter *alcA* immediately after, and oriented towards, the *attR3* recombination sequence. To do so, the *alcA* promoter was PCR-amplified from the *LFY::alcR--alcA::ER-GFP* pGreen vector, digested with *Spe*I and *Hin*DIII and ligated to the pGreen 0229 binary vector, to yield the dpGreenBar-*alcA* binary vector. The *PAN* promoter was PCR-amplified from *Col-0* and recombined with pDONR P4-P1R to yield pPD277. The *PAN-RD* fragment was amplified from pPD269 and recombined with pDONR P2R-P3 to yield pPD317. Finally, the three pENTR vectors (pPD277, pENTR-*alcR*-2xT and pPD317) were recombined into dpGreenBar-*alcA*, to yield the *PAN::alcR--alcA::PAN-RD* binary vector.

The putative bZIP binding sites in the second *AG* intron were identified based on the presence of 'ACGT' core sequences (Jakoby et al., 2002). The six observed sites are (5′-3′): ACTTATACGTACATGT, AGTCCCACGTGATTAC, TTGATCACGTCATCAC, TGTAATACGTATTTGT, TATGGAACGTTGTGAT and TCCATCACGTTTAAAT.

For the *p35S::PAN-VP16* construct, *VP16* was PCR-amplified, digested with *Bam*HI and *Bgl*II, and ligated to pBJ36. The *PAN-VP16* fragment was then PCR-amplified and cloned into the pDONR 221 vector (Invitrogen). The triple gateway system was then used to generate the final p35S::PAN-VP16 plasmid in pdpGreen-BarT. The reporter construct used in the particle bombardment assays, *pAGi-3′*, is published as KB31 (Busch et al., 1999).

Plant lines, transgenics and plant growth conditions

All plants were grown at either 16°C or 22°C with continuous white light, except the *pan-3* and L-*er* plants shown in Fig. S6, which were grown at long days (22°C) under a combination of white and gro-lux light. Photos of flowers were taken using either a Zeiss Stemi SV 11 stereomicroscope fitted with a Zeiss Axiocam or a Leica MZ12 stereomicroscope with a Leica DFC320 camera. Some images were adjusted for clarity by altering the brightness or contrast but any changes were applied evenly, across the entirety of the picture, without exception.

In situ hybridizations were performed according to published protocols. The *WUS* antisense RNA probe corresponds to the entire cDNA. Photos were taken on a Nikon Optiphot-2 equipped with a Zeiss Axiocam.

Transgenic plants were generated using standard floral dipping methods. Transformant lines were selected on soil for resistance to the herbicide Basta. To determine the copy number of the *PAN-RD* transgene, T2 seeds were plated on petri dishes containing 10 μg/ml ammonium glufosinate (Basta) and the ratio of resistant to sensitive seedlings determined (~75% resistant seedlings indicates the parent had a single insertion). The sterile *2×PAN-RD* and *1×PAN-RD pan-2* plants were used as pollen donors to fertilize emasculated wild type flowers, and the F1 seeds were tested as above.

pAP1(*1.7-kb*)-driven expression patterns were assayed in inflorescences of ethanol-induced *pAP1*(*1.7-kb*)*::alcR--alcA::ER-GFP* lines treated with the water soluble lipophilic dye FM4-64 and imaged on a Zeiss 510 confocal microscope.

Chromatin immunoprecipitation

Chromatin immunoprecipitation (ChIP) experiments were performed according to published protocols (Ito et al., 1997). Inflorescences from plants mutant for the redundant *APETALA1* and *CAULIFLOWER* genes, and expressing the dexamethasone-inducible *35S::APETALA-GR* transgene (*p35S::AP1-GR ap1-1 cal-1*), were used. Plants were induced as described (Wellmer et al., 2006) and tissue were collected 5-7 days later for a synchronized population of flowers. Inflorescences were ground in liquid nitrogen, resuspended in buffer M1 (10 mM phosphate buffer 0.1 M NaCl, 10 mM β-mercaptoethanol, 1 M hexylene glycol), fixed with 1% formaldehyde for 10 minutes, washed in buffers M2 [buffer M1 containing 10 mM $MgCl_2$, 0.5% (v/v) Triton X-100] and M3 (10 mM phosphate buffer, 0.1 M NaCl, 10 mM β-mercaptoethanol) and centrifuged to collect nuclei. Chromatin was isolated by resuspending the pellet in lysis buffer [1% SDS (w/v), 10 mM EDTA, 50 mM Tris-HCl pH 8.1] containing protease inhibitors (1 μg/ml Leupeptin, 15 μg/ml Aprotinin), incubating on ice for 10 minutes before adding ChIP dilution buffer (Upstate) supplemented with protease inhibitors. This mixture was sonicated and then pre-cleared with salmon sperm DNA-treated Protein A beads (Upstate) at 4°C for 1-3 hours. The solution was centrifuged, an aliquot of the supernatant kept for use as control for total input DNA (I) and the rest was incubated overnight with anti-PAN antiserum (Chuang et al., 1999) that had been pre-cleared at 4°C for 2 days against leaves and inflorescences from *pan* mutant plants. Chromatin-antibody complexes were captured by incubating with a Protein A slurry at 4°C for 1 hour, centrifuging to remove unbound chromatin and eluting off the beads with elution buffer [1% SDS (w/v), 0.1 M $NaHCO_3$]. Histone-DNA crosslinks were reversed with 0.2 M NaCl at 65°C for 4 hours, RNA and protein were degraded with 40 μg/ml RNase and 40 μg/ml Proteinase K, respectively, and DNA was purified on a standard PCR purification column (Qiagen). This purified, antibody-bound DNA (B) was used to determine enrichment using quantitative real-time PCR on an ABI 7900HT system (Applied Biosystems) with a *MUTATOR-LIKE* (*MU*) locus (At4g03870) serving as control. Relative enrichment levels were calculated by determining the ratio of the 'mean quantity' (calculated by the ABI software) of antibody-bound DNA (B) to total input DNA (I) for the control primers (B_{CTRL}/I_{CTRL}) as well as for each experimental primer pair (B_{EXP}/I_{EXP}), and then normalizing the ratio of the experimental value to the control value [$(B_{EXP}/I_{EXP})/(B_{CTRL}/I_{CTRL})$].

Particle bombardments

Three milligrams of one micron gold microcarrier particles were coated with 2.5 μg of the *p3′AGi* reporter construct alone (for the control) or with an additional 2.5 μg of the *p35S::PAN-VP16* (for the co-bombardments). DNA was premixed prior to each coating. Equal aliquots of the coated particles were then placed onto macrocarriers and bombarded onto onion epidermal cells using a PDS-1000/He Biolistic Particle Delivery System (Bio-Rad) and 1100-psi rupture discs. The onion cells were incubated at 25°C for 2-3 days and then visualized for GUS staining using standard protocols.

RESULTS AND DISCUSSION

A genetic screen uncovers a combined role for *LEAFY* and *PERIANTHIA* in floral stem cell regulation

In a mutagenesis experiment designed to identify modifiers of the floral organ number regulator *PERIANTHIA* (*PAN*) (Chuang et al., 1999; Running and Meyerowitz, 1996), we isolated a new *lfy* allele (see Materials and methods), which we named *lfy-31*. When compared with wild-type flowers (Fig. 1A), *lfy* single mutant flowers (of either *lfy-31* or the well-described *lfy-6* allele) bear organs that resemble leaf-like or sepal-like structures instead of sepals, petals or stamens; and sepalloid organs with stigmatic papillae instead of carpels (Fig. 1B,C). However, flowers of *pan-3* mutants, which we used in the mutagenesis experiment, show no defects in floral identity, but rather bear increased numbers of sepals and petals, and reduced numbers of stamens (Fig. 1D). Flowers of the *pan-3 lfy-31* double mutant line bear several notable differences from flowers of either single mutant. First, the overall number of primary organs is slightly increased with respect to *lfy* flowers (Table 1). Second, whereas the carpelloid structures of *lfy* mutant flowers are fully or partially fused (Fig. 1B,C), those of *pan lfy* flowers remain unfused (Fig. 1E,F). Third, ovule-like structures are often visible within carpels of *lfy* mutants (Fig. 1G) but only very rarely in the *pan lfy* double mutant (Fig. 1F). Finally, whereas all *lfy* flowers produce a determinate number of organs (Weigel et al., 1992), 89% (n=38) of *pan lfy* flowers are indeterminate, such that ectopic floral structures continue to develop interior to the fourth whorl organs (Table 1; Fig. 1F). As a further test of this interaction, we generated lines doubly mutant for *pan-3* and the weak *lfy-5* allele

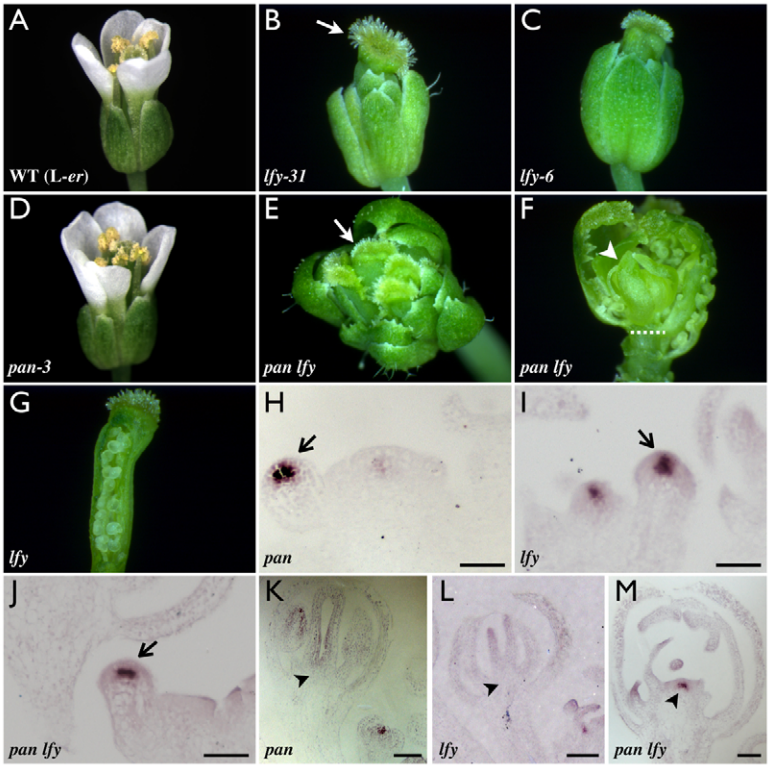

Fig. 1. *pan lfy* double mutant flowers are indeterminate and fail to downregulate *WUS*. (**A-G**) Phenotypes of *pan* and *lfy* single and double mutant flowers. (A) Wild-type flower bearing four sepals, four petals, six stamens and two fused carpels in whorls one to four, respectively. (B) *lfy-31* flower with sepal-like organs in whorls one to three and fused sepalloid/carpelloid organs (arrow) in whorl four. (C) Flower of the well-characterized strong *lfy-6* allele displaying similar phenotypes to *lfy-31*. (D) *pan-3* flower bears extra sepals and petals but no carpel defects. (E) *pan-3 lfy-31* double mutant flower with sepal-like organs in whorls one to three and unfused sepalloid/carpelloid organs (arrow) in whorl four. (F) The same *pan lfy* flower as in E, with several organs removed to expose the ectopic floral structures growing within (arrowhead). The approximate position of the removed fourth-whorl organs is indicated (dotted line). (G) The same *lfy* flower as in B, dissected to reveal a relatively normal gynoecium. (**H-M**) In situ localization of *WUS* transcript in stage 2 flowers (H-J), or in stage 7 or older flowers (K-M), of *pan-3* (H,K); *lfy-6* (I,L); or *pan-3 lfy-31* (J,M) plants. (H-J) Early *WUS* expression (arrows) is similar in all three genotypes. (K-M) In older flowers, no *WUS* expression is observed at the base of the gynoecium (arrowheads) of *pan* (K) and *lfy* (L) single mutants, but remains strong in *pan lfy* flowers (M) of a similar stage. Scale bars: 50 μm.

(Weigel et al., 1992), and observed that these flowers also bear unfused carpels and are indeterminate (see Fig. S1 in the supplementary material). Thus, in plants carrying mutations in both *LFY* and *PAN*, there is an apparent loss of floral determinacy that is not observed in the single mutants alone.

To test the molecular basis of the fourth-whorl phenotypes in *pan lfy* double mutant flowers, we performed in situ hybridization experiments to determine the expression dynamics of the *WUS* transcript, as the downregulation of *WUS* in the stem cell organizing center is essential for floral determinacy (Mayer et al., 1998). As in the case of wild-type flowers (Mayer et al., 1998), *WUS* mRNA is clearly detectable in the center of very early flower buds of *pan-3* and *lfy-6* single mutants, as well as in *pan-3 lfy-31* double mutants (Fig. 1H-J). In the wild type, *WUS* mRNA becomes undetectable by approximately stage 7, when the carpel primordia first appear (Mayer et al., 1998). Similarly, in *pan-3* and *lfy-6* single mutant flowers, *WUS* expression is absent in later-stage flowers (Fig. 1K,L; see Figs S2 and S3 in the supplementary material). By contrast, in older *pan lfy* double mutant flowers, *WUS* expression is clearly detectable within the broad expanse of tissue at the center of the flower from where the organs of the interior floral structures will arise (Fig. 1M; see Fig. S4 in the supplementary material). These results indicate that the indeterminacy phenotypes of *pan lfy* flowers are associated with the persistence of the stem cell pool, as revealed by the continued expression of *WUS* in the stem cell organizing center.

The role of LFY in the center of the floral meristem, via the activation of *AG* expression, has been well studied. In addition, three lines of evidence suggest that PAN might also be active in this region. First, when certain alleles of *pan* (such as *pan-3*) are grown under specific culture conditions (see Materials and methods), some flowers (13%, *n*=84) show slight indeterminacy (see Fig. S5 in the supplementary material). Second, flowers from plants doubly mutant for *pan* and *crabs claw* (the carpel patterning gene) are indeterminate, with a reiteration of carpel structures in internal whorls (see Fig. S6C-F in the supplementary material; Y. Eshed and J. Bowman, personal communication). Third, *pan* mutations restore fourth-whorl carpels to flowers of the *superman-1* (*sup-1*) single mutant that normally either lack carpels or have staminoid carpels, also suggesting a role in this domain (see Fig. S6G-I in the supplementary material) (Running and Meyerowitz, 1996). Because these data reveal a function for PAN in the presumptive fourth whorl, we hypothesized that the determinacy defects apparent in *lfy pan* double mutant flowers were due to a hidden role for PAN in regulating the floral stem cell population, which lies within the fourth whorl.

A dominant-negative *pan* allele induces floral indeterminacy by suppressing *AG* expression

One explanation for the absence of floral indeterminacy phenotypes in most *pan* mutant flowers is that this activity of PAN might be masked by functional redundancy with other factors. To overcome

Table 1. Identities and numbers of organs in *lfy* and *pan* mutant flowers*

Mutant	Sepals/sepal-like	Petals	Stamens	Carpels/sepalloid-carpels	Flowers with interior organs (%)	*n*
pan-3	5.1±0.7	5.1±0.6	5.3±0.7	2	0	77
lfy-6	9.8±0.5	0	0	3.5±0.5	0	40
lfy-31 pan-3	11.2±1.9	0	0	6.9±1.1	89	38

**lfy-6* and *lfy-31 pan-3* flowers were later-arising structures with floral and secondary inflorescence characteristics.

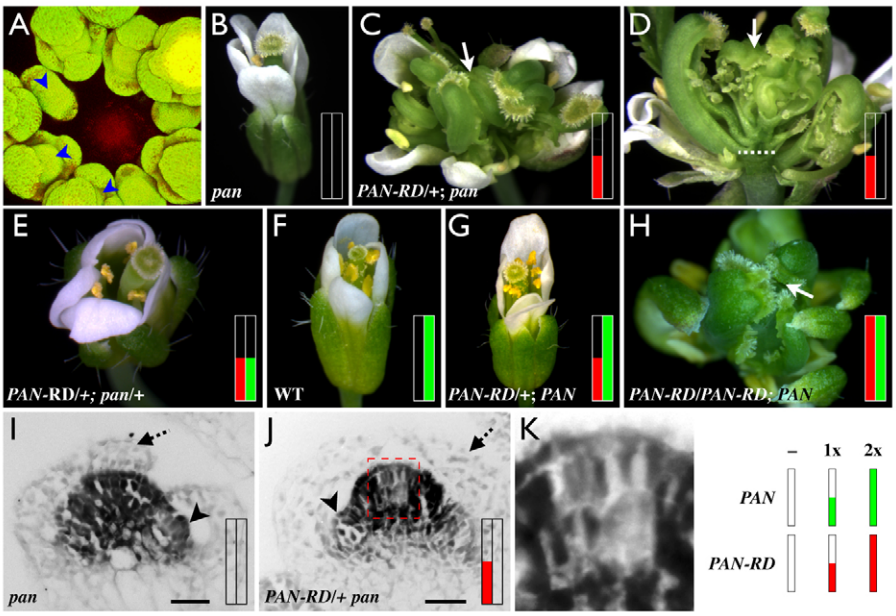

Fig. 2. A dominant-negative *PAN* chimera induces floral determinacy phenotypes. (**A**) *pAP1*(*1.7-kb*)*::alcR--alcA::ER-GFP* expression in an inflorescence meristem. GFP signal (green) is observed in the central domes (arrowheads) of all visible flowers after induction with ethanol vapors. Autofluorescence from the shoot apical meristem is visible (red). (**B-H**) Floral phenotypes of *PAN* wild-type or mutant plants harboring one or more copies of *PAN-RD* under the control of the *AP1*(*1.7-kb*) promoter. Red and green bars indicate the number of copies of *PAN-RD* or wild-type *PAN*, respectively. Open bar indicates no copies, half-filled indicates one copy and filled indicates two copies (see key, bottom right). (B) *pan-2* mutant flower. (C) *pan* flower harboring one copy of *PAN-RD* displaying amplified *pan*-like phenotypes, as well as additional phenotypes such as extra carpels (arrow) and severe floral indeterminacy. (D) Side view of the flower in C with some organs removed to reveal ectopic floral structures (arrow) developing interior to the fourth whorl (demarcated by a dashed line). (E) A *pan*-like phenotype is observed in flowers arising from a cross of genotype in C to wild type. This flower harbors one copy of *PAN-RD* and is heterozygous at the *PAN* locus. (F) Wild-type flower. (G) Wild-type flower harboring one copy of *PAN-RD* displaying a *pan*-like phenotype. (H) Flower from progeny of the plant in G harboring two copies of *PAN-RD* presenting strong indeterminacy defects, similar to *PAN-RD/+ pan* plants (C). (**I-K**) In situ localizations of *AG* transcript in stage 5-6 flowers of *pan-2* (I) or *PAN-RD/+ pan-2* (J,K) plants. *AG* localization appears unperturbed in *pan* flowers (I), but in *PAN-RD/+ pan-2* flowers a central region within the *AG* domain shows diminished signal intensity. Also marked are sepals (dashed arrow) that do not express *AG* and early stamen primordia (arrowhead) that do. (K) Magnified view of the dashed box in J. Scale bars: 10 μm.

such redundancy, we generated a constitutively repressing form of PAN by fusing it to the SUPERMAN repressor domain motif (Hiratsu et al., 2003). Such constructions have been used to study bZIP factors in several model systems (Fukazawa et al., 2000; Rieping et al., 1994) and, in *Arabidopsis*, SUPERMAN repressor domain (RD) fusions of several transcription factors have been shown to phenocopy their corresponding loss-of-function mutants (Baudry et al., 2006; Hiratsu et al., 2003; Xu et al., 2006). The expression of such a *PAN* fusion, either ubiquitously or from the endogenous promoter, yielded plants with severe growth defects, thereby masking any floral phenotypes (data not shown). In order to assay its effects on floral patterning, we thus used the flower-specific *APETALA1* (*AP1*) promoter (Hempel et al., 1997). A 1.7 kb upstream fragment of the *AP1* locus drives expression throughout the early flower; in addition, and at variance with the normal *AP1* expression pattern, it remains active in the entire flower, presumably due to the absence of additional regulatory elements (Fig. 2A; see Fig. S7 in the supplementary material; M. Yanofsky, personal communication).

In order to remove the effects of competition between PAN-RD and endogenous PAN, we introduced the *pAP1*(*1.7-kb*)*::PAN-RD* construct (hereafter referred to as *PAN-RD*) into *pan-2* mutant plants (Fig. 2B). The majority (82%) of these *PAN-RD/+*; *pan/pan* primary transformants bore flowers with increased numbers of petals and stamens (6.3±0.6 and 5.8±0.4 respectively, *n*=20), secondary flowers in the axils of first-whorl organs (2.8±0.6 versus 0 in the wild type and *pan*), extra carpels in the fourth whorl (3.5±0.5) and severe indeterminacy (Fig. 2C,D). The other 18% (*n*=85) of transformants showed a slight enhancement of the *pan* organ number phenotypes without any determinacy defects (data not shown). To eliminate the possibility that the indeterminacy phenotypes were caused by the use of the *AP1*(*1.7-kb*) promoter fragment, we used an ethanol-inducible two component system (Deveaux et al., 2003; Maizel and Weigel, 2004) to drive *PAN-RD* expression under the endogenous *PAN* promoter. In the absence of induction, *pan-2* plants bearing this construct show no fourth-whorl phenotypes (see Fig. S8A in the supplementary material). However, after induction with ethanol, we observe flowers bearing unfused gynoecia and ectopic internal carpel structures (see Fig. S8B in the supplementary material). Thus, expression of a PAN-repressor domain fusion protein in the flower leads to the loss of floral determinacy, a phenotype observed at low frequency in *pan* mutant plants grown in specific culture conditions (see above).

A caveat to the use of dominant-negative alleles is that they may act as neomorphs, altering the expression of ectopic, rather than genuine, downstream targets of the protein under study. We decided to study this by varying the ratio of chimeric to wild-type protein. If *PAN-RD* behaves as a true dominant-negative allele, increasing doses of it should yield increasingly stronger phenotypes, whereas increasing doses of unmodified *PAN* should attenuate the phenotypes. We first

used pollen from the *PAN-RD/+*; *pan/pan* flowers described above in a cross to wild type and examined the phenotypes of F1 plants selected for the presence of the transgene. We found that these flowers (*PAN-RD/+*; *pan/+*) had phenotypes similar to the *pan* mutant (compare Fig. 2E with 2B). Thus the same *PAN-RD* insertion that confers strong indeterminacy phenotypes on *pan* flowers does not do so on *pan/+* heterozygotes (instead yielding only the more sensitive organ number defect), showing that *PAN-RD* expression does not ectopically induce floral indeterminacy. Next we examined primary transformants in wild-type plants, thus with two additional wild-type copies of *PAN* (Fig. 2F). Approximately 20% (n=60) of these plants (genotypically *PAN-RD/+*; *PAN/PAN*) phenocopied the *pan* mutant (Fig. 2G; 4.3±0.5 sepals, 4.9±0.3 petals and 4.7±0.5 stamens; n=20), whereas the rest showed no discernable phenotypes. We then examined the progeny of these plants, to determine the phenotypes of plants harboring two copies of the transgene (see Materials and methods). These flowers (*PAN-RD/PAN-RD*; *PAN/PAN*) displayed strong phenotypes, including extra carpels and floral indeterminacy (Fig. 2H), and closely resembled *PAN-RD/+*; *pan/pan* flowers (Fig. 2C,D). Taken together, these data show that the effects of the PAN-RD fusion protein are modified by wild-type PAN in a dosage sensitive manner. This suggests that PAN-RD and endogenous PAN compete for the same targets and that the *PAN-RD* phenotypes are due to the repression of genuine PAN targets.

To characterize the molecular basis of the *PAN-RD* phenotype, we performed in situ hybridizations to determine whether the *PAN-RD* transgene induced changes in *AG* expression patterns. We observed that, as in the wild type, *AG* is expressed uniformly throughout the third and fourth whorls of stage 5-6 *pan-2* flowers (Fig. 2I). However, in similarly staged *PAN-RD/+*; *pan/pan* flowers, *AG* expression is patchy, with the central region of the floral meristem showing reduced expression (Fig. 2J,K). Since *pAP1*(*1.7-kb*) drives expression throughout the central dome of the flower during these stages, these results indicate that the PAN-RD chimera might exert an unequal influence on different cells within the *AG*-expressing region.

Thus our results show that expression of a PAN-RD fusion protein in the flower is sufficient to mimic *pan* loss-of-function phenotypes and to produce floral indeterminacy. Since the indeterminacy phenotype occurs more stably in *PAN-RD* plants than in *pan* simple mutants, this role possibly requires other spatially or temporally restricted factors. Taken together with the phenotypes of the double mutant flowers described above, this suggests that PAN plays a role in the development of the fourth whorl, specifically in the proper regulation of the floral stem cell population, and that this role is achieved through the regulation of *AG*. Furthermore, as the effects of *PAN-RD* were similar to the loss-of-function phenotypes of *pan* mutant alleles, the role of PAN in floral determinacy is likely to be that of an activator of a gene involved in the process.

PAN binds *AG* regulatory sequences in vivo

We next sought to determine the precise mechanism by which PAN affects floral stem cell fate. As discussed above, AG is a key regulator of this process, by itself acting to repress *WUS* expression. Because *AG* expression is perturbed in *PAN-RD* flowers and because PAN is a predicted transcriptional activator, we reasoned that its role might be to positively regulate *AG* expression. To test whether PAN directly associates with the *AG* promoter, we used chromatin immunoprecipitation (ChIP) assays, which examine the in vivo binding of transcription factors to DNA. We maximized the sensitivity of our assays by using a synchronized population of flowers at stages 5-7 (Wellmer et al., 2006) (see Materials and methods), as the stem cell organizing activity is known to be terminated during this time. In addition, we used a characterized PAN-specific polyclonal antibody that, when used in immunohistochemical analyses, detects protein signals closely resembling *PAN* mRNA expression patterns, but showing no signal in mutant flowers (Chuang et al., 1999). We further pre-cleared this antibody against tissue from *pan-2* plants prior to immunoprecipitating intact protein-DNA complexes. We then performed quantitative real-time RT-PCR to assay for the enrichment of sequences within the 3 kb second intron of the *AG* locus with respect to input DNA, where important cis regulatory sequences are located (Fig. 3A) (Busch et al., 1999; Deyholos and Sieburth, 2000; Hong et al., 2003; Lohmann et al., 2001; Parcy et al., 1998; Sieburth and Meyerowitz, 1997). We observed that five amplicons out of a total of eight tested within this region are significantly enriched (Fig. 3B; amplicons B=9.2-fold±2.0, C=9.0±0.6, F=6.6±0.7, G=4.9±0.4 and H=40.5±9.2) when

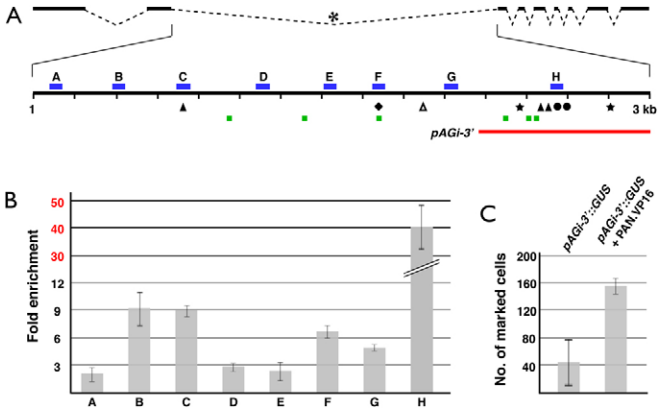

Fig. 3. PAN directly binds *AGAMOUS* regulatory sequences. (**A**) Structure of the 5.7 kb *AG* locus. Exons and introns (top) are represented in bold and dashed lines, respectively. The second intron (asterisk) contains all known *AG* regulatory elements. The detailed view of the 3 kb intron shows the fragments used to determine enrichment in the chromatin immunoprecipitation assays (blue bars), the 3′ fragment used in co-bombardment experiments (red line), and evolutionarily conserved elements and known or predicted transcription factor binding motifs (Davies et al., 1999; Hong et al., 2003; Lohmann et al., 2001; Parcy et al., 1998). Black triangles, LFY/WUS binding sites; white triangle, predicted LFY binding site; stars, CArG boxes; circles, CCAAT boxes; diamond, AAGAAT motif; green squares, predicted core bZIP binding sites; vertical tick marks: 200 bp intervals. (**B**) Results of chromatin immunoprecipitation experiments from stage 5-7 flowers. Anti-PAN antiserum was used to isolate protein-DNA complexes and DNA enrichment levels were measured by quantitative real-time RT-PCR (see Materials and methods). Enrichment was calculated for antibody-bound DNA relative to total input DNA and was then normalized against an internal genomic control. Vertical bars show mean enrichment levels from duplicate experiments for amplicons distributed along the intron (shown in 3A). The scale for amplicon 'H' is different and is shown in red. Results are shown only for amplicons with a coefficient of correlation (r^2)>0.98. (**C**) Results of particle co-bombardment experiments in onion epidermal cells. Vertical bars represent mean values from duplicate experiments for numbers of cells stained for GUS enzymatic activity. The *pAGi-3′::GUS* reporter, which recapitulates most facets of *AG* expression in vivo, shows some background activity (left bar) in onion epidermal cells. When co-bombarded with *p35S::PAN-VP16* (right bar), the 'numbers of cells' stained for GUS activity is 4- to 5-fold greater. Error bars represent standard deviation from the mean.

normalized relative to internal genomic controls. These data demonstrate that PAN, either alone or in a complex, binds *AG* regulatory sequences in vivo.

Because of the nature of ChIP assays, not every enriched fragment necessarily contains a PAN binding site. Four of the five ChIP-enriched amplicons (B, C, F and H) map to regions previously described as being very highly conserved (Hong et al., 2003). Of these, amplicon C contains binding sites for LFY and WUS (Lohmann et al., 2001; Parcy et al., 1998), whereas predicted bZIP core binding sites (Jakoby et al., 2002) are located within or close to two others (F and H). Hong et al. (Hong et al., 2003) have shown that an *AG* reporter containing a deletion within amplicon H loses expression at later floral stages, suggesting that it plays a role in the maintenance of *AG* expression. In an accompanying article (Maier et al., 2009), the authors use one-hybrid assays to show that amplicon F contains PAN binding sites. Furthermore, they show that mutations in this bZIP motif disrupt binding in vitro and eliminate in vivo expression in the context of an *AG* reporter. Given the very high enrichment of amplicon H in our ChIP assays, we were interested in determining whether this region might also contain PAN binding sites. To this end, we made use of a published 3′ *AG* reporter construct that reproduces the normal *AG* expression pattern in vivo (Busch et al., 1999). In this reporter, an 800 bp 3′ *pAG* fragment (Fig. 3A) drives expression of the *uidA* gene, which encodes the β-glucuronidase (GUS) enzyme (Busch et al., 1999). We performed particle co-bombardment experiments in onion epidermal cells with a putative constitutively activated form of *PAN* (*p35S::PAN-VP16*). Although the reporter alone presents basal reporter activity in onion cells (44.5±34.6 cells; Fig. 3C; see Fig. S9A,C in the supplementary material), perhaps due to the presence of minimal *p35S* sequences, 4- to 5-fold greater numbers of cells (157±11.3; Fig. 3C; see Fig. S9B,D in the supplementary material) show GUS activity when co-bombarded with *p35S::PAN-VP16*. It is thus possible that PAN has two or more target sites within the *AG* promoter, to which it might bind with different affinities or different partners.

Flowers mutant for *AG* display stem cell overproliferation phenotypes and, in addition, also show homeotic transformations of stamens to petals (Bowman et al., 1989). Since *PAN-RD* disrupts floral stem cell regulation without inducing the homeotic transformations associated with the loss of *AG* function, we asked whether PAN might function as a general regulator of *AG*, or only to modify its activity in the fourth whorl. To this end, we used the weak *ag-4* allele, which produces flowers with reduced numbers of stamens and with fourth whorl organs replaced by another flower (Fig. 4A) (Sieburth et al., 1995). Mutations in several loci, including *HUA1* and *HUA2*, *REBELOTE* (*RBL*) or *ULTRAPETALA1* (*ULT1*) enhance the *ag-4* allele by fully or partially converting stamens to petals (Chen and Meyerowitz, 1999; Fletcher, 2001; Prunet et al., 2008). We reasoned that if PAN plays a general role in regulating *AG* expression, a *pan* allele might similarly enhance the weak *ag* phenotype. Conversely, if PAN participates primarily in the floral determinacy aspects of *AG*, the double mutant might not be significantly enhanced. In fact, we observe that *pan-2 ag-4* double mutant flowers (Fig. 4B) differ from *ag-4* single mutants only in that they present an additional *pan*-like phenotype: extra perianth organs (4.8±0.5 sepals and 4.8±0.5 petals compared with four each in *ag-4*; n=20 for both genotypes), as is the case for double mutants of *pan* and the strong *ag-1* allele (Running and Meyerowitz, 1996). The third-whorl stamens of *pan-2 ag-4* flowers appear morphologically normal, although they are reduced in number (5.5±0.5 compared with 5.8±0.4 in *ag-4*). This suggests either that the stamen identity functions of the mutant protein encoded by the *ag-4* allele are robust and are not perturbed by the absence of PAN, or that PAN regulates *AG* expression only in the fourth whorl.

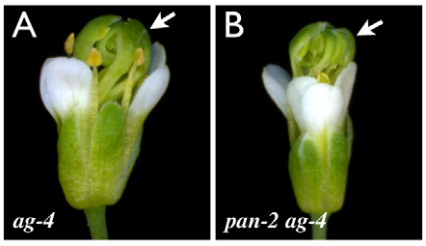

Fig. 4. *pan* mutations do not enhance the third-whorl phenotypes of a weak *ag* allele. (**A**) Flower of the weak *ag-4* allele in a mixed background of wild-type accessions (L-*er*/*Ws*). Such flowers have normal outer organs but fourth-whorl carpels are replaced with a new flower (arrow). (**B**) A *pan-2 ag-4* flower in the same genetic background has the altered floral organ numbers of the *pan* mutant and the new fourth-whorl flower phenotype of *ag-4* (arrow).

Prunet et al. (Prunet et al., 2008) have recently proposed the existence of a distinct subdomain within the floral fourth whorl, in which a decrease in *AG* expression is sufficient to disrupt the specification of floral determinacy. Two observations indicate that the effects of PAN on the *AG* promoter might be spatially restricted, perhaps to this subdomain. First, in *PAN-RD* flowers, there is a marked reduction in the accumulation of *AG* transcript at the very center of the dome of the floral meristem. Second, unlike many other *AG* interactors (Chen and Meyerowitz, 1999; Fletcher, 2001; Prunet et al., 2008), *pan* mutations have no effect on the third whorl phenotypes of a weak *ag* allele. A restricted effect of PAN on *AG* expression might explain why mutations in *PAN* attenuate the fourth whorl phenotype of *sup* mutants (Running and Meyerowitz, 1996), which produce reduced or masculinized carpels (see Fig. S6G,H in the supplementary material) (Bowman et al., 1992). One model is that in the center of the fourth whorl of *pan sup* double mutant flowers (see Fig. S6I in the supplementary material), even the mild reduction in *AG* expression caused by the absence of PAN could lead to increased or prolonged *WUS* expression, and thus to an increase in the size of this region. Since the stamen identity genes *AP3* and *PI* are excluded from the very center of *sup* flowers (Bowman et al., 1992; Goto and Meyerowitz, 1994), the corresponding, but enlarged, region in *pan sup* flowers could now become specified into a functional carpel.

Like *PAN*, the broadly expressed *APETALA2* (*AP2*) gene, the absence of which causes only specific floral phenotypes (a change in sepal and petal identities), was recently shown, through the characterization of a semi-dominant allele, to play a role in the control of stem cells in the shoot (Würschum et al., 2006). Thus both PAN and AP2 have primary roles in specific aspects of floral patterning, but also have masked functions in stem cell regulation that are likely to require interactions with other domain- and/or stage-specific factors. Identifying these interactors through genetic screens or other methods could prove invaluable in gaining a full understanding of the complex regulatory mechanisms that control stem cell fate.

As the main function of AG in floral determinacy appears to be to downregulate *WUS* expression in a narrow temporal window, *AG* expression must be quickly upregulated in order to ensure the complete arrest of stem cell fate, and thereby ensure proper floral

patterning. We suggest that plants have evolved a complex, multiply redundant system to ensure the proper regulation of *AG*, and furthermore, that many of the factors involved in the regulation of floral stem cells probably also perform unrelated patterning functions.

We thank J. Lohmann for sharing unpublished results; Arnavaz Garda, Alexis Lacroix, Claudia Bardoux and Hervé Leyral for technical assistance; Ioan Negrutiu, Christophe Trehin, Nathanaël Prunet and Olivier Hamant for useful discussions and comments on the manuscript; Ioan Negrutiu for sharing unpublished results and seeds; and John Bowman and Marty Yanofsky for communicating unpublished results. This work was supported by a Caltech Division of Biology postdoctoral fellowship (to P.D.), a Marie Curie Incoming International Fellowship IIF-022002 (to P.D.), the EU Marie Curie SY-STEM Network (to J.T.) and a NSF Grant IOS-0544915 (to E.M.M.).

Supplementary material

Supplementary material available online at
http://dev.biologists.org/cgi/content/full/136/10/1605/DC1

References

Baudry, A., Caboche, M. and Lepiniec, L. (2006). TT8 controls its own expression in a feedback regulation involving TTG1 and homologous MYB and bHLH factors, allowing a strong and cell-specific accumulation of flavonoids in *Arabidopsis thaliana*. *Plant J.* **46**, 768-779.

Bowman, J. L., Smyth, D. R. and Meyerowitz, E. M. (1989). Genes directing flower development in *Arabidopsis*. *Plant Cell* **1**, 37-52.

Bowman, J. L., Sakai, H., Jack, T., Weigel, D., Mayer, U. and Meyerowitz, E. M. (1992). *SUPERMAN*, a regulator of floral homeotic genes in *Arabidopsis*. *Development* **114**, 599-615.

Busch, M. A., Bomblies, K. and Weigel, D. (1999). Activation of a floral homeotic gene in *Arabidopsis*. *Science* **285**, 585-587.

Chen, X. and Meyerowitz, E. M. (1999). *HUA1* and *HUA2* are two members of the floral homeotic *AGAMOUS* pathway. *Mol. Cell* **3**, 349-360.

Chuang, C. F., Running, M. P., Williams, R. W. and Meyerowitz, E. M. (1999). The *PERIANTHIA* gene encodes a bZIP protein involved in the determination of floral organ number in *Arabidopsis thaliana*. *Genes Dev.* **13**, 334-344.

Davies, B., Motte, P., Keck, E., Saedler, H., Sommer, H. and Schwarz-Sommer, Z. (1999). *PLENA* and *FARINELLI*: redundancy and regulatory interactions between two *Antirrhinum* MADS-box factors controlling flower development. *EMBO J.* **18**, 4023-4034.

Deveaux, Y., Peaucelle, A., Roberts, G. R., Coen, E., Simon, R., Mizukami, Y., Traas, J., Murray, J. A., Doonan, J. H. and Laufs, P. (2003). The ethanol switch: a tool for tissue-specific gene induction during plant development. *Plant J.* **36**, 918-930.

Deyholos, M. K. and Sieburth, L. E. (2000). Separable whorl-specific expression and negative regulation by enhancer elements within the *AGAMOUS* second intron. *Plant Cell* **12**, 1799-1810.

Eshed, Y., Baum, S. F., Perea, J. V. and Bowman, J. L. (2001). Establishment of polarity in lateral organs of plants. *Curr. Biol.* **11**, 1251-1260.

Fletcher, J. C. (2001). The *ULTRAPETALA* gene controls shoot and floral meristem size in *Arabidopsis*. *Development* **128**, 1323-1333.

Fukazawa, J., Sakai, T., Ishida, S., Yamaguchi, I., Kamiya, Y. and Takahashi, Y. (2000). REPRESSION OF SHOOT GROWTH, a bZIP transcriptional activator, regulates cell elongation by controlling the level of gibberellins. *Plant Cell* **12**, 901-915.

Gleave, A. P. (1992). A versatile binary vector system with a T-DNA organisational structure conducive to efficient integration of cloned DNA into the plant genome. *Plant Mol. Biol.* **20**, 1203-1207.

Goto, K. and Meyerowitz, E. M. (1994). Function and regulation of the *Arabidopsis* floral homeotic gene *PISTILLATA*. *Genes Dev.* **8**, 1548-1560.

Hempel, F. D., Weigel, D., Mandel, M. A., Ditta, G., Zambryski, P. C., Feldman, L. J. and Yanofsky, M. F. (1997). Floral determination and expression of floral regulatory genes in *Arabidopsis*. *Development* **124**, 3845-3853.

Hiratsu, K., Matsui, K., Koyama, T. and Ohme-Takagi, M. (2003). Dominant repression of target genes by chimeric repressors that include the EAR motif, a repression domain, in *Arabidopsis*. *Plant J.* **34**, 733-739.

Hong, R. L., Hamaguchi, L., Busch, M. A. and Weigel, D. (2003). Regulatory elements of the floral homeotic gene *AGAMOUS* identified by phylogenetic footprinting and shadowing. *Plant Cell* **15**, 1296-1309.

Ito, T., Takahashi, N., Shimura, Y. and Okada, K. (1997). A serine/threonine protein kinase gene isolated by an in vivo binding procedure using the Arabidopsis floral homeotic gene product, AGAMOUS. *Plant Cell Physiol.* **38**, 248-258.

Jakoby, M., Weisshaar, B., Droge-Laser, W., Vicente-Carbajosa, J., Tiedemann, J., Kroj, T. and Parcy, F. (2002). bZIP transcription factors in *Arabidopsis*. *Trends Plant Sci.* **7**, 106-111.

Laux, T., Mayer, K. F., Berger, J. and Jurgens, G. (1996). The WUSCHEL gene is required for shoot and floral meristem integrity in Arabidopsis. *Development* **122**, 87-96.

Lenhard, M., Bohnert, A., Jurgens, G. and Laux, T. (2001). Termination of stem cell maintenance in *Arabidopsis* floral meristems by interactions between *WUSCHEL* and *AGAMOUS*. *Cell* **105**, 805-814.

Lohmann, J. U., Hong, R. L., Hobe, M., Busch, M. A., Parcy, F., Simon, R. and Weigel, D. (2001). A molecular link between stem cell regulation and floral patterning in *Arabidopsis*. *Cell* **105**, 793-803.

Maier, A. T., Stehling-Sun, S., Wollmann, H., Demar, M., Hong, R. L., Haubeiß, S., Weigel, D. and Lohmann, J. U. (2009). Dual roles of the bZIP transcription factor PERIANTHIA in the control of floral architecture and homeotic gene expression. *Development* **136**, 1613-1620.

Maizel, A. and Weigel, D. (2004). Temporally and spatially controlled induction of gene expression in *Arabidopsis thaliana*. *Plant J.* **38**, 164-171.

Mayer, K. F., Schoof, H., Haecker, A., Lenhard, M., Jurgens, G. and Laux, T. (1998). Role of *WUSCHEL* in regulating stem cell fate in the *Arabidopsis* shoot meristem. *Cell* **95**, 805-815.

Mizukami, Y. and Ma, H. (1995). Separation of *AG* function in floral meristem determinacy from that in reproductive organ identity by expressing antisense *AG* RNA. *Plant Mol. Biol.* **28**, 767-784.

Parcy, F., Nilsson, O., Busch, M. A., Lee, I. and Weigel, D. (1998). A genetic framework for floral patterning. *Nature* **395**, 561-566.

Prunet, N., Morel, P., Thierry, A. M., Eshed, Y., Bowman, J. L., Negrutiu, I. and Trehin, C. (2008). *REBELOTE*, *SQUINT*, and *ULTRAPETALA1* function redundantly in the temporal regulation of floral meristem termination in *Arabidopsis thaliana*. *Plant Cell* **20**, 901-919.

Rieping, M., Fritz, M., Prat, S. and Gatz, C. (1994). A dominant negative mutant of PG13 suppresses transcription from a cauliflower mosaic virus 35S truncated promoter in transgenic tobacco plants. *Plant Cell* **6**, 1087-1098.

Running, M. P. and Meyerowitz, E. M. (1996). Mutations in the *PERIANTHIA* gene of *Arabidopsis* specifically alter floral organ number and initiation pattern. *Development* **122**, 1261-1269.

Schultz, E. A. and Haughn, G. W. (1991). *LEAFY*, a homeotic gene that regulates inflorescence development in *Arabidopsis*. *Plant Cell* **3**, 771-781.

Sieburth, L. E. and Meyerowitz, E. M. (1997). Molecular dissection of the *AGAMOUS* control region shows that *cis* elements for spatial regulation are located intragenically. *Plant Cell* **9**, 355-365.

Sieburth, L. E., Running, M. P. and Meyerowitz, E. M. (1995). Genetic separation of third and fourth whorl functions of AGAMOUS. *Plant Cell* **7**, 1249-1258.

Weigel, D. and Meyerowitz, E. M. (1993). Activation of Floral Homeotic Genes in *Arabidopsis*. *Science* **261**, 1723-1726.

Weigel, D., Alvarez, J., Smyth, D. R., Yanofsky, M. F. and Meyerowitz, E. M. (1992). *LEAFY* controls floral meristem identity in *Arabidopsis*. *Cell* **69**, 843-859.

Wellmer, F., Alves-Ferreira, M., Dubois, A., Riechmann, J. L. and Meyerowitz, E. M. (2006). Genome-wide analysis of gene expression during early *Arabidopsis* flower development. *PLoS Genet.* **2**, e117.

Würschum, T., Gross-Hardt, R. and Laux, T. (2006). *APETALA2* regulates the stem cell niche in the *Arabidopsis* shoot meristem. *Plant Cell* **18**, 295-307.

Xu, Y., Teo, L. L., Zhou, J., Kumar, P. P. and Yu, H. (2006). Floral organ identity genes in the orchid *Dendrobium crumenatum*. *Plant J.* **46**, 54-68.